Critical behavior of thermal parameters at the smectic-*A*−hexatic-*B* and smectic-*A*−smectic-*C* phase transitions in liquid crystals

F. Mercuri, M. Marinelli, and U. Zammit
INFM and Università di Roma "Tor Vergata," via del Politecnico 1, 00133 Rome, Italy

C. C. Huang
Department of Physics, University of Minnesota, Minneapolis, Minnesota 55455, USA

D. Finotello
Department of Physics, Kent State University, Kent, Ohio 44242, USA

High temperature resolution measurements of thermal conductivity, thermal diffusivity, and specific heat, with simultaneous polarized light visual inspection of the sample, have been performed at two different liquid crystal phase transitions: the Sm*A*-Sm*C* (Smectic-*A*−Smectic-*C*) and the Sm*A*-Hex*B* (Smectic-*A*−hexatic-*B*) in racemic A7 [4-(3-methyl-2-chlorobutanoyloxy)-4′-heptyloxybiphenyl] and 65OBC (*n*-hexyl-4′-*n*-pentyloxybiphenyl-4-carboxylate) compounds, respectively. In the past, anomalies in the thermal conductivity at the transitions have been reported. Our results indicate a nonsingular behavior of the thermal conductivity at both transitions, similarly to what has been previously reported for the smectic-*A*−nematic phase transition. It is also shown how, in several cases, the nature of the transition can be affected by the sample thermal history due to the presence of strain annealing phenomena.

I. INTRODUCTION

The smectic-*A*−nematic (*AN*), smectic-*A*−smectic-*C* (*AC*), and the smectic-*A*−hexatic-*B* (*AB*) phase transitions in liquid crystals have been extensively studied in recent years. It has been predicted that such transitions can be continuous and all of them were indicated to belong to the 3D (three-dimensional) *XY* universality class for the critical fluctuations [1]. Experimentally there are indications confirming such hypothesis for the *AN* transition in samples with wide enough nematic range (see, for instance Ref. [2], and references therein) while for the *AC* one, experimental results have shown [3] that it can be well described in terms of extended mean-field theory. According to Safyna *et al.* [4], this is possible because the bare correlation length of the fluctuations at the *AC* transition is so large that the critical region becomes experimentally inaccessible. The nature of the *AB* transition seems not as yet well established and shows a critical behavior ruled by peculiar values of the critical quantities. For the specific heat critical exponent α, for instance, values from $\alpha = 0.48$ to $\alpha = 0.68$ are reported in literature [5–10] while the measured values for the order parameter exponent β are in the range 0.15–0.25 [11–13] being in both cases very different from $\alpha_{XY} = -0.007$ and $\beta_{XY} = 0.345$, respectively [14,15], predicted by the 3D *XY* model.

Concerning the presence of a tricritical point, it has been well established that the *AN* transition shows a crossover to a tricritical behavior which is characterized by the value $\alpha = 0.5$ [2,16] and the *AC* transition has been shown to go through a mean-field tricritical point [17–20]. In both cases such a crossover can be associated with a decreasing temperature range of the nematic phase for the *AN* transition or

the smectic-*A* phase for the *AC* one. The picture is less clear for the *AB* transition and for the possibility to determine its predicted [7,21,22] tricritical point. It was initially assumed for this transition that the large measured values of the specific heat *c* critical exponent, close to 0.5, could be taken as an indication of the tricritical behavior. But neither a continuous crossover from the 3D *XY* to tricritical behavior nor a connection between the α values and the width of the less ordered phase [5] could be found even though it has been definitely shown that the *AB* transition may be first order [7–9].

The situation seems even more confusing in dynamics where very few measurements of thermal transport parameters are available in literature and their theoretical interpretation appears inadequate. A number of recently published papers reported on the behavior of the thermal transport parameters at the *AN* [and also at the nematic-isotropic (*NI*)] phase transition in liquid crystals [23]. In all studied compounds the thermal conductivity *k* is never found to show either critical behavior or pretransitional effects, suggesting that its behavior is dominated by short range processes [24]. In contrast, the behavior of the thermal diffusivity $D = k/\rho c$ (ρ is the sample density) at the transition temperatures shows a critical slowing down which is due to the anomaly in the specific heat. An anomaly in *k* [6] and a divergence in *D* [25] have, on the other hand, been observed at the *AB* and at the *AC* phase transitions, respectively, and an explanation of the results, based on critical dynamic theories, has been proposed. Moreover, sharp peaks have also been observed in the *k* behavior at the *AN* transition for different cyanobiphenyl compounds [26,27] but no physical explanation was provided. In this latter case, improvements in the experimental technique led the same authors to conclude that the observed

anomalies were likely artifacts arising from thermal gradients present in the sample [23].

In this paper we have performed under different experimental conditions an analysis of the k, D, and c behavior at the AC and AB phase transitions of the racemic A7 [4-(3-methyl-2-chlorobutanoyloxy)-4′-heptyloxybiphenyl] and 65OBC (n-hexyl-4′-n-pentyloxybiphenyl-4-carboxylate) compounds, respectively. Our goal is to arrive at a more complete picture and understanding the nature of all those phase transitions at which anomalies in the thermal transport parameters have been reported. For this purpose we have exploited the capabilities of the photopyroelectric (PPE) technique as it allows the simultaneous determination of k, c, and D, and also the possibility of cell wall treatment creating a preferred direction for molecular alignment. In addition, we have monitored the liquid crystal textures by visual inspection with polarized light during the high resolution measurements [27,28].

In what follows we present a study of the thermal transport parameters over wide temperature range showing how, at the AB and AC transitions, the sample thermal history can affect the nature of the transition itself. We show that, after the A7 sample enters the SmA-CrG transition region, even when not achieving completely the final crystal-G structure, during the subsequent heating run the PPE signal amplitude and phase from which the thermal parameters are extracted showed a peculiar behavior across the AC transition different from that obtained when cooling the sample across the transition itself. Such a behavior is not observed when scanning the temperature up and down across the AC transition region as long as the sample is not cooled enough to reach crystal-G phase. A similar sample thermal history dependence of the PPE signal is also observed for the 65OBC compound at the AB transition where the peculiar behavior of the amplitude and phase was observed only during the first cooling run from the isotropic phase. These results suggest that the anomalous behaviors associated with the sample thermal history are due to processes of strain annealing. Further, it will be shown that the amount of strain present in the liquid crystal mesophase can be affected by the action of external ordering fields as, for example, that due to the cell walls. Finally, we show that in the absence of such strain annealing, the thermal conductivity does not show any critical behavior over both the AB and the AC transitions similarly to what occurs at the AN transition. This indicates that in all the phase transitions in liquid crystals where the critical behavior of the thermal conductivity has been studied (also including the nematic-isotropic transition), there are no anomalies in the thermal conductivity across the phase transition.

II. EXPERIMENTAL METHOD AND RESULTS

The experimental setup used is the standard photopyroelectric working in its back detection configuration that has been fully described elsewhere [27]. In the current measurements, the sample has a thickness of 30 μm, and is sandwiched between the titanium coated glass cover and the transparent pyroelectric sensor which is coated on both sides with transparent indium-tin oxide (ITO) electrodes. Since the
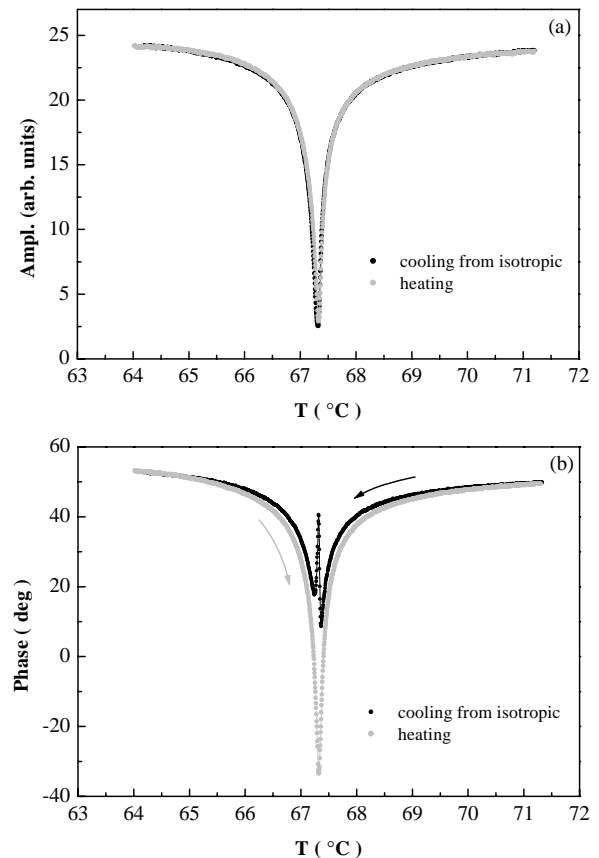
FIG. 1. Amplitude (a) and phase (b) behavior of the PPE signal at the AB transition of the 65OBC compound.

sample confining surfaces are electrically conductive, an external electric field can also be applied to the sample along the direction of heat propagation in order to influence the molecular alignment. In addition, along the same direction, a polarized light beam is allowed to propagate through the transparent sensor and the liquid crystal sample and is reflected by the titanium layer at the bottom of the cell. The emerging beam goes through an analyzer and reaches a charge-coupled device camera. The images are recorded during the PPE high resolution measurements so that the sample texture can be monitored by polarized light and related to the thermal parameters behavior at all temperatures investigated [28].

A. Results on 65OBC

One of the studied compounds is 65OBC which melts into the hexatic-B phase at 62.6 °C, becomes smectic-A at 67.7 °C and isotropic at 83.7 °C. On cooling its phase transition sequence is I-(83.7 °C)-SmA-(67.7 °C)-Hex$B$-(60.3 °C)-CrE-(52.7 °C)-K. Concerning the AB transition of this compound, it has recently been suggested by the work of Haga *et al.* [8], to be weakly first order.

Cooling the 65OBC sample from the isotropic phase with a temperature rate change of 20 mK/min, we obtained for PPE signal amplitude and phase, the black dot curves reported in Fig. 1. The focal conic texture of the corresponding smectic-A phase obtained under these conditions is shown in
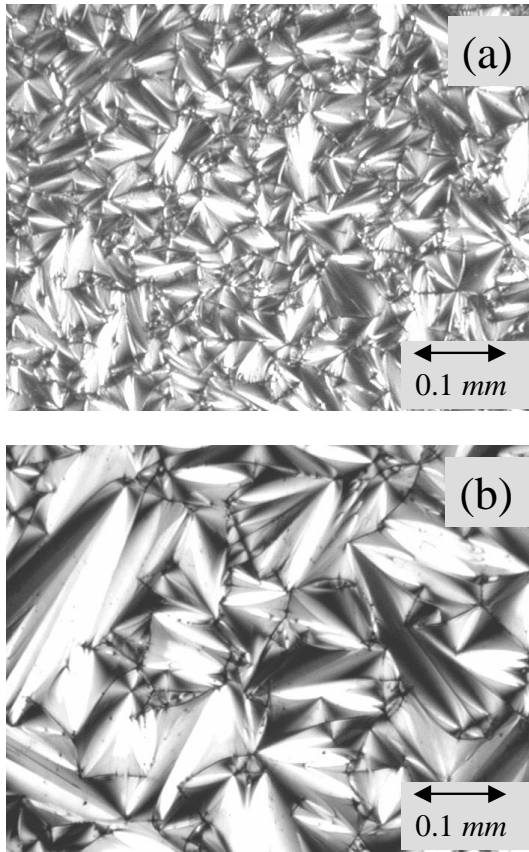
FIG. 2. SmA focal conic textures observed at $T = 69\,°C$ in the 65OBC compound when cooling the sample from the isotropic phase. Across the I-SmA transition temperature: (a) rate $= 20$ mK/min, no external field applied; (b) rate$= 1$ mK/min, cell walls treated with surfactant, electric field of $1\ V/\mu m$ rms applied.

Fig. 2(a). In Fig. 1, the light gray dot curves have been obtained from the subsequent heating run, inverting the direction of the temperature change at $64\,°C$, well inside the Hex$B$ phase. Continuing cycling the sample temperature between $64\,°C$ and $71.5\,°C$, all subsequent heating and cooling curves perfectly reproduce the original heating run of Fig. 1. By comparing heating and cooling measurements, Figs. 1(a) and 1(b), it can be noted that the two signal amplitude values differ slightly at their minima at the AB transition while the phase shows a completely different behavior between them, with a peak appearing over the phase transition when cooling the sample from the isotropic phase. An analogous observation was reported in Ref. [8], where, when cooling the sample from the isotropic phase, the specific heat curves showed some anomalies that were interpreted as due to strain present in the material.

In order to better investigate the possible role of the strain, we have repeated in our sample the cooling measurement from the isotropic phase under conditions such as to increase the domain size in the material which should correspond to a reduction of strain. Figure 2(b) shows the focal conic texture of the SmA phase obtained after the sample was cooled more slowly (1 mk/min), the cell walls were treated by a surfactant so as to try to induce a preferred molecular orientation, and an external electric field

($1\ V/\mu m$) was applied to the sample during the smectic-A phase onset. Under these conditions, the focal conic domains are of a much larger dimension and the PPE signal amplitude and phase curves fully reproduce starting with the first cooling run. The shapes are those seen in Fig. 1 for the first heating run, and do not have the anomalous peak in the phase. We believe this to further indicate that strain in the material affects the nature of the AB transition giving rise to the appearance of the anomalous peak in the PPE signal phase. Therefore, we have determined the thermal parameters behavior for the AB phase transition from the PPE signal amplitude and phase dataset corresponding to the light gray dots in Fig. 1. The results for c, k, and D are reported in Fig. 3 and discussed below.

1. Specific heat

Following a standard approach to second-order fluctuation-dominated transitions for 3D XY systems, we fitted the specific heat data to a power law expression. Although the AB transition in the 65OBC compound, as already mentioned, can be taken to be weakly first order [8], a power law expression can be successfully used in this case if one allows the critical contribution of the c regular behavior (defined below) to be different below and above T_C. We have therefore fitted our specific heat data to the expression

$$c = B^{\pm} + E(T - T_C) + A^{\pm}|T - T_C|^{-\alpha} \qquad (1)$$

referring, here and hereafter, $+$ and $-$ to $T > T_C$ and $T < T_C$, respectively.

The $B^{\pm}$ parameter is defined by the expression $B^{\pm} = B_b + B_C^{\pm}$, where $B_C^{\pm}$ represent the critical contribution to the c regular behavior and B_b is the constant term of the specific heat noncritical background $c_b = B_b + E(T - T_C)$. In Fig. 3(a) the specific heat data are shown together with the black solid line curve corresponding to the value parameters obtained by fit 2 of Table I. The fit quality is good ($\chi^2 = 0.999$) and it should be pointed out that no improvement is obtained introducing into the fitting expression (1) the correction to scaling term $1 + D^{\pm}|T - T_C|^{0.75}$ as used in previous work at the same transition [5,8].

In order to check the first-order nature of this transition, we fitted the specific heat data introducing the constrain $B^- = B^+$ (that is to say $B_C^- = B_C^+$). The results are reported in fit 2 of Table I. The fit quality is relatively poor ($\chi^2 = 1.425$) and could not be improved even by introducing a correction-to-scaling term in the fitting expression. Imposing $B_C^- = B_C^+$ makes impossible to get a fit quality comparable with that of fit 1, indicating the presence of a step discontinuity at T_C and, consequently, the first-order nature of the transition.

A final remark concerns the reduced temperature range selected for data fitting. Fits 1 and 2 in Table I (as well as fits 3, 5, 6 and, in Table III, fit 13) have been performed for $|t| < |t|_{max} = 1.1 \times 10^{-2}$. When the fitted data region is extended up to $|t|_{max} = 2.1 \times 10^{-2}$, no substantial changes are introduced in the fitting parameters values.
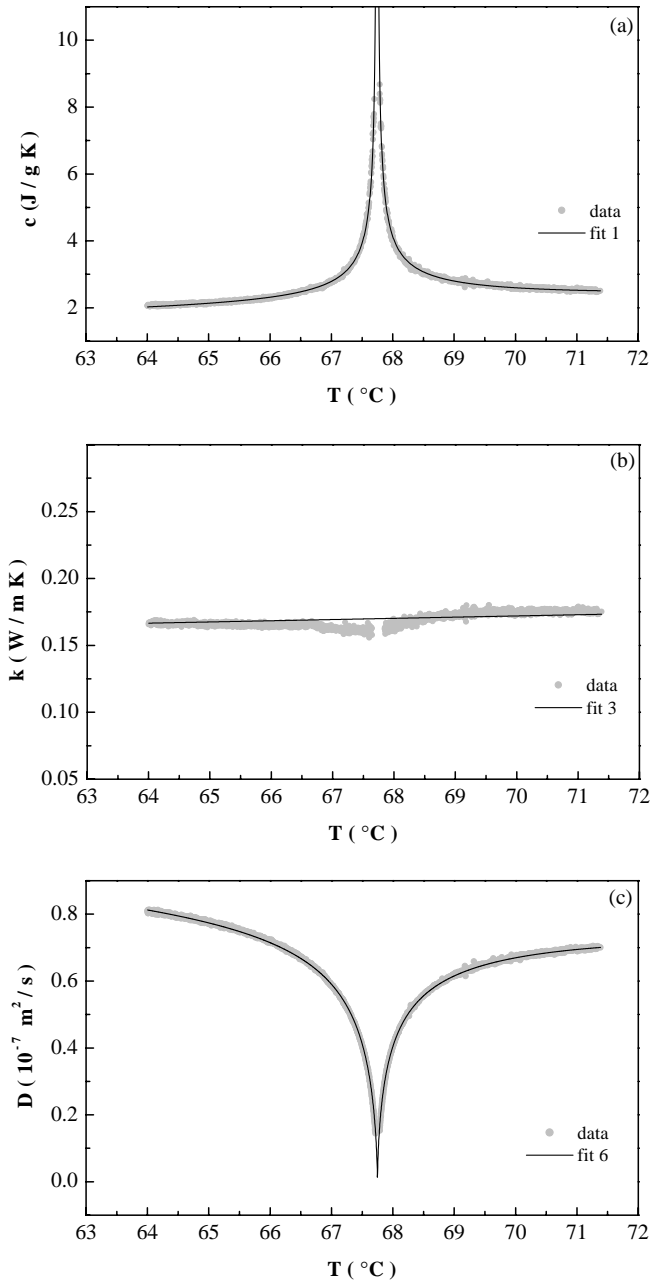
FIG. 3. (a) Specific heat, (b) thermal conductivity, and (c) thermal diffusivity vs temperature in the 65OBC compound over the AB transition.

2. Thermal conductivity

Figure 3(b) shows the thermal conductivity data at the AB transition for the 65OBC compound. There is no singular behavior of k, rather it seems to linearly depend on temperature. We therefore decided to fit the thermal conductivity data to the expression

$$k = H + G(T - T_C). \tag{2}$$

Fit 3 in Table I is the best fit obtained for the k data using expression (2), and is plotted by the continuous black line in

Fig. 3(b). Fit 4, obtained by fitting a different measurement, will be discussed later on in this paper.

3. Thermal diffusivity

The evidence that the k data can be fitted with a linear temperature dependence supports the idea that thermal conductivity behavior is nonsingular across the AB transition. It also suggests that the anomaly in the thermal diffusivity is simply related to the specific heat critical behavior. Considering the fundamental relation among thermal parameters $k = D/\rho c$, and hereafter assuming $\rho = 10^6$ g/m^3, the D data was fit to the expression

$$D = [H + G(T - T_C)]/[B^{\pm} + E(T - T_C) + A^{\pm}|T - T_C|^{-\alpha}]. \tag{3}$$

The thermal diffusivity data are plotted in Fig. 3(c) with the continuous line representing the best fit curve corresponding to fit 6 of Table I. We had first tried to fit data (fit 5) fixing the values of the H and G parameters to those found in fit 3. The fit quality was good and the free parameter values were substantially in agreement with those from fit 1. However, releasing all fixed parameters (fit 6) leads to a significant improvement of the χ^2 value (from 1.710 to 1.065) while, at the same time, all the obtained parameter values remain very close to those obtained with fits 1 and 3.

B. Results for racemic A7

The racemic A7 compound is obtained by mixing 50% of the d and l enantiomer. On heating it melts into the smectic-A phase at 75 °C and becomes isotropic at about 82 °C. On cooling its phase transition sequence is I-(82.10 °C)-SmA-(72.50 °C)-SmC-(70.25 °C)-CrG. The AC transition is continuous and basically corresponds to the mean-field tricritical point [17].

We started the analysis of racemic A7 sample by studying the PPE signal vs temperature from which the thermal parameters behavior can be obtained. In Fig. 4 the light gray dots curves represent the PPE signal amplitude and phase vs temperature, obtained when cooling the sample from the isotropic phase. Both amplitude and phase exhibit a dip at the transition temperature. If the sample is prevented from reaching the CrG phase, the PPE signal is reproduced in all the subsequent heating and cooling cycles across the transition temperature.

When on the other hand the sample is heated from the crystal-G phase to the temperature region of the smectic phases, the PPE signal amplitude and phase curves are different from those obtained in the cooling run. In particular, the amplitude shows a greater value at its minimum at the transition while the phase shows a peak at the transition and its values in the smectic-C phase are larger than those obtained when cooling the sample from the isotropic phase. The subsequent cooling run from the SmA phase shows that the PPE signal amplitude and phase curves reproduce the light gray dot run in Fig. 4 (no peak in the signal phase) as did all the subsequent heating and cooling cycles across the transition temperature provided, once again, that the sample

TABLE I. Parameters values for fitting c, k, and D data in the 65OBC compound over the AB transition temperature region. Fits 1, 2, 3, 5, 6 have been obtained on a reduced temperature range t having $|t|_{max} = 1.1 \times 10^{-2}$. Fit 4 has been obtained from dataset which is a different from the other ones, and on a t range that has $|t|_{max} = 1.9 \times 10^{-2}$. Units of E, $A^{\pm}$, and G obtained assuming $(T - Tc)$ as a dimensionless quantity (i.e., divided by 1 K).

	Fit	B^- (J/gK)	B^+ (J/gK)	E (J/gK)	A^- (J/gK)	A^-/A^+	α	T_C (°C)	H (W/mK)	G (W/mK)	χ^2
c	1	1.793 ±0.004	2.050 ±0.004	0.030 ±0.001	0.836 ±0.002	1.010 ±0.003	0.671 ±0.009	67.745 ±0.001			0.999
	2	1.942 ±0.005	(B^-)	0.0717 ±0.0006	0.769 ±0.005	0.906 ±0.008	0.681 ±0.002	67.745 ±0.001			1.425
k	3							67.745 (Fixed)	0.169 ±0.001	9×10^{-4} ±2×10^{-4}	1.309
	4							67.745 (Fixed)	0.171 ±0.002	5×10^{-4} ±2×10^{-4}	1.211
D	5	1.802 ±0.004	2.021 ±0.004	0.028 ±0.001	0.864 ±0.004	1.037 ±0.007	0.689 ±0.005	67.745 ±0.001	0.169 (Fixed)	9×10^{-4} (Fixed)	1.710
	6	1.795 ±0.004	2.019 ±0.004	0.026 ±0.008	0.897 ±0.005	1.063 ±0.009	0.687 ±0.009	67.745 ±0.001	0.170 ±0.004	7×10^{-4} ±4×10^{-4}	1.065

is prevented from reaching the CrG phase .

Figures 5(a–c) represent the sequence of textures shown by the racemic A7 sample when cooling it from the isotropic phase to the crystal-G, and Figs. 5(d) and 5(e) the subse-

quent heating to the smectic-A phase. Typical smectic-A focal conic [Fig. 5(a)] and smectic-C focal conic broken fan [Fig. 5(b)] textures are exhibited by the sample during the first cooling run from the isotropic phase. Further cooling leads to the onset of the crystal-G phase whose mosaic texture is shown in Fig. 6(c). When the sample is heated above the CrG melting temperature, its texture is characterized by a pattern which basically reproduces the crystal-G one with the superposition of striations. In this stage, the PPE signal phase values are found to be larger than the values obtained in the same temperature range when cooling from the isotropic phase. We take this to indicate that the SmC phase was not properly formed. Upon heating the sample further to its smectic-A phase the texture continues to show the same background pattern but the striations are now absent. The PPE signal amplitude and phase values, however, are now the same as those obtained when cooling the sample from the isotropic phase, thus showing this to be a true smectic-A phase. We therefore believe that the peak in the PPE signal

FIG. 4. (a) Amplitude and (b) phase behavior of the PPE signal at the AC transition of the racemic A7 compound.
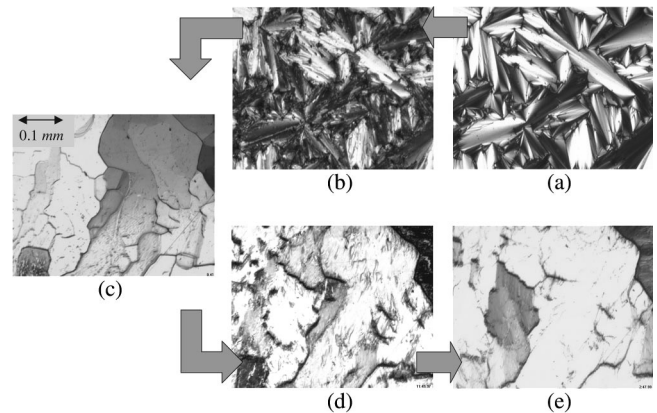
FIG. 5. Textures observed in different phases for the racemic A7 compound during sample cooling [(a) SmA at $T = 77$ °C, (b) SmC at $T = 72$ °C, and (c) CrG at $T = 68$ °C] and during subsequent heating [(d) at $T = 72$ °C and (e) at $T = 77$ °C].
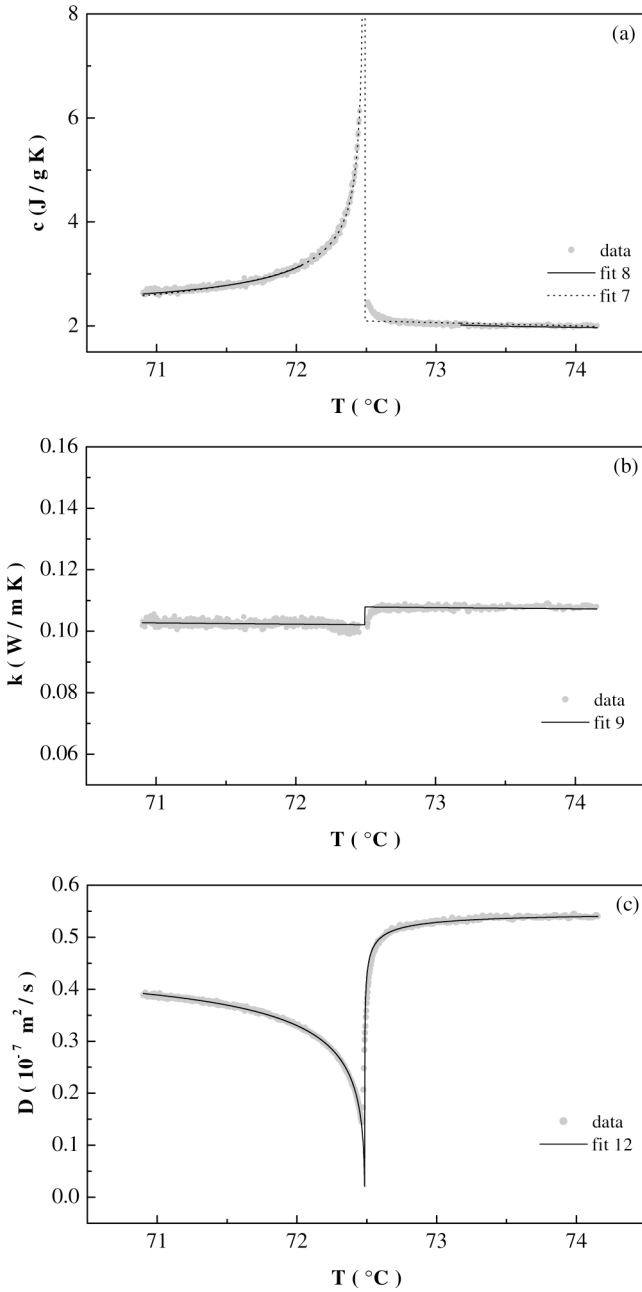
FIG. 6. (a) Specific heat, (b) thermal conductivity, and (c) thermal diffusivity vs temperature in the racemic A7 compound over the AC transition.

phase observed when heating the sample from the crystal-G phase does not reflect the true nature of the AC transition, similar to what occurred at the AB transition. As further discussed later on, a possible explanation is that the phase that forms after melting from CrG is excessively defective and a real SmC order can be obtained in the sample only when cooling it from the SmA phase.

For this racemic A7 compound, we have also determined the thermal parameters behavior at the AC transition from the PPE signal amplitude and phase curves that show no peak in the phase over the transition, i.e., when cooling the sample from the isotropic phase. The results for c, k, and D are reported in Fig. 6 and described below.

1. Specific heat

As previously mentioned, the AC transition is supposed to belong to the 3D XY universality class and a heliumlike critical behavior may be expected. Nevertheless, if we look at the specific heat data in Fig. 6(a), the abrupt jump shown by the c anomaly in the high temperature side of the transition seems to be the characteristic of mean-field-like transitions. In fact, it has been shown that the c behavior at AC transition of the A7 compound can be fitted to

$$c = c_0 \quad (T > T_C), \tag{4}$$

$$c = c_0 + AT|T_m - T|^{-1/2} \quad (T < T_C), \tag{5}$$

obtained from the extended mean-field model [3] where, in the Landau expansion of the free energy

$$f = f_0 + at\,\theta^2 + b\,\theta^4 + c\,\theta^6, \tag{6}$$

the sixth-order term is included. In expression (6), a, b, and c are the expansion coefficients, θ is the director tilt angle which represents the order parameter for the AC transition, f_0 is the nonsingular part of f, and $t = (T - T_C)/T_C$ is the reduced temperature with T_C the transition temperature. In the fitting expressions (4) and (5), $A = \sqrt{a^3/12c(T_C)^3}$ and $T_m = T_C(1 + t_0/3)$, where $t_0 = b^2/ac$ is a quantity characterizing the excess specific heat sharpness at the AC transition and whose value depends on how close the transition is to the tricritical point (when $b = 0$). Finally, $c_0 = B + Et$ is the f_0 contribution to the specific heat with B and E the two parameters that characterize the nonsingular c linear background. It must be noted that on both side of the transition temperature pretransitional fluctuations effects are present in the c curve that are not taken into account in the above extended mean-field expressions (4) and (5). So, unlike in previously reported results for A7, we included the Gaussian fluctuation terms, $c_g^+ = c_g(T/T_C)^2|t|^{-1/2}$ and $c_g^- = (1/2\sqrt{2})c_g(T/T_C)^2|t|^{-1/2}$, in the fitting expressions. The expressions for such terms were derived from a more generalized model also valid for thin films [29] and after using suitable scaling laws [30].

Fit 7 has been obtained with expressions (4) and (5) and the corresponding curve is represented by the dotted line plotted in Fig. 6(a). It is clear, particularly for $T > T_C$, that the fit quality is poor, as also stressed by the corresponding large value of $\chi^2 = 2.963$. Fit 8 has been obtained with the expressions

$$c = c_0 + c_g(T/T_C)^2|t|^{-1/2} \quad (T > T_C), \tag{7}$$

$$c = c_0 + AT|T_m - T|^{-1/2} + (1/2\sqrt{2})c_g(T/T_C)^2|t|^{-1/2}$$

$$(T < T_C). \tag{8}$$

The corresponding fit curve is shown in Fig. 6(a), by the continuous line. The fit quality has now greatly improved and that is confirmed by a value of $\chi^2 = 1.005$.

TABLE II. Parameters values for fitting c, k, and D data in the racemic A7 compound over the AC transition temperature region. All the fits have been obtained on a reduced temperature range t having $|t|_{max} = 4.5 \times 10^{-3}$.

	Fit	B (J/gK)	E (J/gK)	A (J/gK$^{3/2}$)	T_m (°C)	T_C (°C)	c_g (J/gK)	H^- (W/mK)	H^+ (W/mK)	G (W/mK)	χ^2
c	7	2.097	-21.8	2.14×10^{-3}	72.486						2.963
		± 0.002	± 0.4	$\pm 0.01 \times 10^{-3}$	± 0.002						
	8	1.936	-6.04	2.31×10^{-3}	72.493	72.490	4.13×10^{-3}				1.005
		± 0.002	± 0.05	$\pm 0.02 \times 10^{-3}$	± 0.002	± 0.001	$\pm 0.05 \times 10^{-3}$				
k	9							0.1022	0.1076	-0.05	1.395
								± 0.0001	± 0.0001	± 0.03	
	10							0.1021	0.1079	-0.14	1.114
								± 0.0001	± 0.0001	± 0.04	
D	11	1.927	-6.7	2.31×10^{-3}	72.490	72.486	4.7×10^{-3}	0.1021	0.1079	-0.14	1.144
		± 0.005	± 0.5	$\pm 0.01 \times 10^{-3}$	± 0.003	± 0.02	$\pm 0.9 \times 10^{-3}$	(Fixed)	(Fixed)	(Fixed)	
	12	1.94	-7	2.13×10^{-3}	72.487	72.486	4.7×10^{-3}	0.1002	0.1085	-0.19	1.095
		± 0.03	± 1	$\pm 0.02 \times 10^{-3}$	± 0.005	± 0.02	$\pm 0.9 \times 10^{-3}$	± 0.0008	± 0.0008	± 0.05	

2. Thermal conductivity

In Fig. 6(b) we present the thermal conductivity data that, also in this case, do not show any critical behavior at the AC transition temperature. The k dependence on temperature seems approximately linear with a very small jump at T_C. The data was fit to the expression

$$k = H^\pm + Gt. \qquad (9)$$

Fit 9 of Table II lists the values obtained for the fitting parameters $H^\pm$ and G; the solid line in Fig. 6(b) represents the corresponding fitting curve. The fit quality is rather good except for few data in the temperature range (~ 50 mK) just above T_c where the k value rapidly increases by about 5%. Such a jump in the k value may be explained in terms of molecular reorientation in the vicinity of the AC transition. In the SmA phase, which forms cooling down the sample from the isotropic phase, due to the effect of the cell walls, the orientation of the smectic planes may eventually not be purely random. During the onset of the smectic phase, the molecules may tend to align preferably normal to the cell walls with the smectic planes parallel to them. This effect, even if very weak, could be responsible for a nonzero component of the average director of the sample molecules in the direction perpendicular to the cell walls. Entering the SmC phase, molecules tilting can make the k value slightly vary. We therefore tried to fit the thermal conductivity excluding those data belonging to that temperature region (fit 10) and found an appreciable improvement in the fit quality ($\chi^2 = 1.114$).

A final remark concerns the possibility to have different values of the G parameter for $T < T_C$ and $T > T_C$, respectively. Fitting the k data to the expression $H^\pm + G^\pm t$, allowing G^- to be different from G^+, the best fits are always obtained for G values that are the same below and above T_C.

3. Thermal diffusivity

Once more, the nonsingular character of the k behavior across the critical region suggests to fit the thermal diffusivity data to the following expressions:

$$D = (H^- + Gt)/(c_0 + c_g^-) \quad (T > T_C), \qquad (10)$$

$$D = (H^+ + Gt)/(c_0 + AT|T_m - T|^{-1/2} + c_g^+) \quad (T < T_C), \qquad (11)$$

given by the simple ratio of the k to c expressions.

In fit 11 of Table II the $H^\pm$ and G parameter values have been fixed to those obtained from fit 10. The fit quality is good and improves when all the parameters are released. The result is reported in fit 12 and the corresponding curve is shown by the solid line in Fig. 6(c). All values obtained for the fitting parameters agree well, as expected, with those obtained by fitting k and c separately.

III. DISCUSSION

In the case of the AB transition, in order to explain the existing discrepancy between the 3D XY nature predicted for that transition and the experimental results so far reported in the literature, such a system has been proposed [8] to be a quasitricritical one. The quasitricritical nature would be originated from the coupling between the amplitude of hexatic order parameter $|\Psi|$ and the in-plain position density or strain. Quasitricriticality implies for the system to always have a first-order character even if very weak. In this respect the question about which is the order of the AB transition in the 65OBC compound, considered in the past as either first or second order, becomes relevant.

We have shown how in the analysis of our specific heat data that our best data fits have been obtained with $\Delta B \equiv \Delta B_C = B_C^+ - B_C^- > 0$. That represents, according to Ref. [8], the first-order character of the transition. In particular, from our best c and D fits we have obtained $\Delta B_1 = 0.257$ Jg^{-1} K^{-1} and $\Delta B_6 = 0.224$ Jg^{-1} K^{-1} (the indice refer to the number of the corresponding fit). Similar values ranging from 0.157 Jg^{-1} K^{-1} up to 0.208 Jg^{-1} K^{-1} we found in Ref. [8]. In order to have a more significant comparison with the results in Ref. [8], we reanalyzed our specific heat data following the approach used therein. First, from the c data over a wide temperature range, we extracted
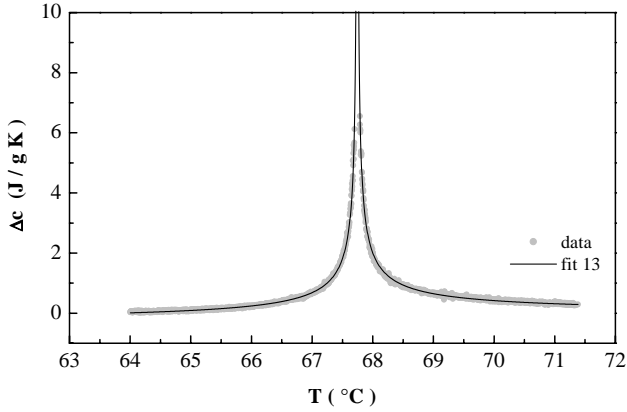
FIG. 7. Excess specific heat vs temperature in the 65OBC compound over the AB transition obtained by subtracting the nonsingular background c_b from the specific heat data reported in Fig. 3(a).

its noncritical background $c_b = B + E(T - T_C)$. The temperature range considered was 20 °C, from 61 °C (just above the CrE-Hex$B$ transition temperature) up to 81 °C, well within the smectic-A phase. The obtained specific heat background, taking $T_C = 67.745$ °C, is

$$c_b = [2.12 + 0.0265(T - T_C)] \ \mathrm{Jg^{-1} \ K^{-1}}. \qquad (12)$$

Subtracting such a background from our specific heat data, we obtained the excess specific heat Δc plotted in Fig. 7 where the solid black line represents the fit curve corresponding to the parameters values listed in fit 13 of Table III. From such a very good quality fit we obtained $\Delta B_{13} = 0.276 \ \mathrm{Jg^{-1} \ K^{-1}}$, very close to the values determined from the previous fits to c and D and similar to those of Ref. [8]. In conclusion, the results of our c data analysis support a weakly first-order nature of the AB transition in the 65OBC compound.

Concerning the hypothesis of a quasitricritical nature of such a system, if we assume that it can be due to an in-plane coupling between $|\Psi|$ and the strain [8], it should not be surprising that strain annealing phenomena related to the onset of the transition from the smectic-A to hexatic-B phases could affect the nature of the transition itself. In that respect, the anomaly shown just below T_C by the PPE signal phase curve [Fig. 1(b)] during the first sample cooling from the isotropic phase could be related to some strain annealing processes relative to the onset of the in-plane short positional order. The detection of a similar annealing phenomena was also described in Ref. [8] where a small anomalous rounded peak in the c vs T curve was observed at a 5×10^{-5} reduced

temperature distance below the transition temperature and annealed when cycling the temperature over the AB transition. In that case it was assumed that the strain was associated with contraction in the material upon ordering in the hexatic-B phase due to the reduced lateral intermolecular distance in hexatic-B 65OBC. It was argued that cycling around the transition temperature produced progressive annealing of the strain due to the in-plane increase of the correlation length $\xi_\parallel$ in the hexatic-B phase giving rise to short range but well correlated regions combined with regions that are more disordered. Similar annealing of surface induced strain upon cycling has also been reported in 65OBC [31]. The occurrence of such annealing may be reflected in changes in PPE signal phase not associated with thermal diffusivity changes but to, for example, enthalpy release. As stated earlier on, further indication that the anomalous peak in the PPE signal phase may be associated with strain in the material, is the fact that such peak can be reduced or removed altogether when strain is decreased by increasing the domain size in the material.

Concerning the racemic A7 compound, the specific heat behavior at the AC transition has been shown to be well described by an extended mean-field model. The fitting expressions (7) and (8) for c, where the Gaussian fluctuation terms are included, give excellent fits to our dataset. Due to the presence of the $c_g^{\pm}$ terms in the fitting expression, in addition to T_m, T_C is also a fit parameter. That makes it possible to have a straightforward indication of the tricritical character of the transition from the evaluation of $t_0 = 3(T_m - T_C)/T_C$. Using the T_m and T_C values of fit 8, a very small value of $t_0 = 3 \times 10^{-5}$ is obtained revealing the proximity of the transition to a tricritical point. Such a value of t_0 is in agreement with published results [18].

As already mentioned, an important point in the investigation of the properties of the A7 compound is represented by the initial condition of the sample determined by its previous thermal history as also shown in the case of 65OBC compound. At the AC transition, when the sample is heated starting from the CrG phase, the value of the amplitude at its minimum over the phase transition, is considerably larger than the one obtained in the previous cooling run [Fig. 4(a)]. The phase shows a sharp peak [Fig. 4(b)] which is no longer observed in the subsequent cooling and heating runs unless the sample is allowed again to enter the crystal-G phase.

Considering the peak in the PPE signal phase over both the AB and AC transitions, assuming the condition of validity of the theoretical model for the analysis of the PPE signal is satisfied (a homogeneous sample, no latent heat involved

TABLE III. Parameters values for fitting the excess specific heat for the 65OBC compound over the AB transition. Fits 13 has been obtained on the same reduced temperature range t of fits 1, 2, 3, 5, 6. Units of $A^{\pm}$ obtained assuming $(T - Tc)$ as a dimensionless quantity (i.e., divided by 1 K).

	Fit	B_c^- (J/gK)	B_c^+ (J/gK)	A^- (J/gK)	A^-/A^+	α	T_C (K)	χ^2
$\Delta c = c - c_b$	13	-0.331 ± 0.002	-0.055 ± 0.004	0.832 ± 0.002	1.016 ± 0.003	0.674 ± 0.004	67.745 ± 0.002	0.993

and therefore that changes in the signal phase are only due to changes in thermal diffusivity) we would expect a peak in the thermal diffusivity and a consequent peak also in the thermal conductivity, as reported in Ref. [6] for the AB transition and in Ref. [25] for the AC one. A possible explanation for differences with published results concerning the critical behavior of k and D and this study, may be connected with those samples affected by thermal history effects in the material associated with strain annealing phenomena which at the time of those measurements were not known and thus could not be prevented.

Our results clearly indicate that for both the AC and the AB transitions the thermal conductivity is nonsingular at T_C while the thermal diffusivity shows a dip simply related to the specific heat anomaly. The behavior of k across the transition is independent of the critical behavior of c and D, only depending on their backgrounds. To verify this conclusion, similarly to what was done for the specific heat, we extracted from the thermal diffusivity, the nonsingular background

$$D_b = U + W(T - T_C) \qquad (13)$$

from the measurement performed in 65OBC over the more extended temperature range that allows a reliable determination of the background. This background was combined with c_b according to the relation $k = \rho c_b D_b$, and compared to the curve of the thermal conductivity data. Considering $T_C = 67.745\,°C$, we obtain

$$D_b = [0.811 - 7.8 \times 10^{-3}(T - T_c)] \times 10^{-7}\ m^2\ s^{-1}, \quad (14)$$

which, when combined with expression 12, and assuming $\rho = 10^6$ g/m^3, gives

$$k = \rho c_b D_b = H + G(T - T_C)$$
$$= [0.171 + 5 \times 10^{-4}(T - T_c)]\ Wm^{-1}\,K^{-1}, \qquad (15)$$

where nonlinear terms have been neglected. The k curve obtained (not reported) results are basically indistinguishable from those of fit 3 seen in Fig. 6(b). The values of the coefficients H and G in expression (15) are very close to those obtained in fit 3 in the more reduced temperature range, and nearly coincide with those obtained by fitting the k data belonging to the more extended temperature range previously mentioned (fit 4), where the backgrounds for the specific heat and thermal diffusivity have been calculated.

Finally, for the behavior of k across the AC transition in the racemic A7 compound, some doubts remain about the origin of the small discontinuity observed at T_C. We believe that our explanation, based on molecular reorientation arguments, needs to be more thoroughly investigated. It may be possible to vary the assumed nonzero residual component of the average molecular director by means of external fields or, alternatively, to minimize it by using much thicker cells. In the latter case, in fact, the effect of the cell walls would be negligible and the sample would be expected to form a perfectly random polydomain in the smectic-A phase; k would show no discontinuity at T_C.

IV. CONCLUSIONS

The main issue we have addressed in this work is whether the thermal conductivity can be singular at a liquid crystal phase transition. We have found that, unlike in previously reported results, the thermal conductivity shows no anomalous behavior across the AB and AC phase transitions, in analogy with reports for the AN and NI transitions. In particular, the thermal diffusivity simply shows a critical slowing down related to the excess specific heat.

We have also found that the thermal history of the sample can affect the behavior of the observed quantities across the AB and AC phase transitions in connection to strain annealing that under certain conditions takes place in the sample.

Finally, for the studied A7 and 65OBC compounds, we also presented specific heat measurements and relative data analysis over the AB and AC transitions, respectively, confirming the first-order nature of the transition in the first case and including Gaussian fluctuations in the data analysis in the second case.

---

[1] P.G. de Gennes, Mol. Cryst. Liq. Cryst. **21**, 49 (1973).

[2] C.W. Garland and G. Nounesis, Phys. Rev. E **49**, 2964 (1994).

[3] C.C. Huang and J.M. Viner, Phys. Rev. A **25**, 3385 (1982).

[4] C.R. Safiyna, M. Kaplan, J. Als-Nielsen, R.J. Birgeneau, D. Davidov, J.D. Litster, D.L. Johnson, and M. Neubert, Phys. Rev. B **21**, 4149 (1980).

[5] T. Pitchford, G. Nounesis, S. Dumrongrattana, J.M. Viner, C.C. Huang, and J.W. Goodby, Phys. Rev. A **32**, 1938 (1985).

[6] G. Nounesis, C.C. Huang, and J.W. Goodby, Phys. Rev. Lett. **56**, 1712 (1986).

[7] C.C. Huang, G. Nounesis, R. Geer, J.W. Goodby, and D. Guillon, Phys. Rev. A **39**, 3741 (1989).

[8] H. Haga, Z. Kutnjak, G.S. Iannacchione, S. Qian, D. Finotello, and C.W. Garland, Phys. Rev. E **56**, 1808 (1997).

[9] H. Haga and C.W. Garland, Phys. Rev. E **57**, 603 (1998).

[10] C.C. Huang, and T. Stoebe, Adv. Phys. **42**, 343 (1993).

[11] E. Gorecka, L. Chen, W. Pyzuk, A. Krowczynski, and S. Kumar, Phys. Rev. E **50**, 2863 (1994).

[12] E. Gorecka, L. Chen, A. Lavrentovich, and W. Pyzuk, Europhys. Lett. **27**, 507 (1994).

[13] C. Rosenblatt and J.T. Ho, Phys. Rev. A **26**, 2293 (1982).

[14] C. Bagnuls and C. Bervillier, Phys. Rev. B **32**, 7209 (1985).

[15] J.C. Le Guillon and J. Zinn Justin, J. Phys. (Paris), Lett. **46**, L137 (1985).

[16] K.J. Stine and C.W. Garland, Phys. Rev. A **39**, 3148 (1989).

[17] H.Y. Liu, C.C. Huang, Ch. Bahr, and G. Heppke, Phys. Rev. Lett. **61**, 345 (1988).

[18] J. Boerio-Goates, C.W. Garland, and R. Shashidhar, Phys. Rev. A **41**, 3192 (1990).

[19] Ch. Bahr and G. Heppke, Phys. Rev. Lett. **65**, 3297 (1990).

[20] T. Chan, Ch. Bahr, G. Heppke, and C.W. Garland, Liq. Cryst. **13**, 667 (1993).

[21] R. Bruinsma and G. Aeppli, Phys. Rev. Lett. **48**, 1625 (1982).

[22] A. Aharony, R.J. Birgeneau, J.D. Brock, and J.D. Litster, Phys. Rev. Lett. **57**, 1012 (1986).

[23] (a) M. Marinelli, F. Mercuri, U. Zammit, and F. Scudieri, Phys. Rev. E **53**, 701 (1996); (b) M. Marinelli, F. Mercuri, S. Foglietta, U. Zammit, and F. Scudieri, *ibid.* **54**, 1604 (1996); (c) F. Mercuri, U. Zammit, and M. Marinelli, *ibid.* **57**, 596 (1998).

[24] M. Marinelli, F. Mercuri, U. Zammit, and F. Scudieri, Phys. Rev. E **58**, 5860 (1998).

[25] E.K. Hobbie, H.Y. Liu, C.C. Huang, Ch. Bahr, and G. Heppke, Phys. Rev. Lett. **67**, 1771 (1991).

[26] U. Zammit, M. Marinelli, R. Pizzoferrato, F. Scudieri, and S. Martellucci, Phys. Rev. A **41**, 1153 (1990).

[27] M. Marinelli, U. Zammit, F. Mercuri, and R. Pizzoferrato, J. Appl. Phys. **72**, 1096 (1992).

[28] F. Mercuri, M. Marinelli, and U. Zammit, Appl. Phys. Lett. **81**, 4148 (2002).

[29] L. Reed, T. Stoebe, and C.C. Huang, Phys. Rev. E **52**, R2157 (1995).

[30] S.K. Ma, *Modern Theory of Critical Phenomena* (Benjamin-Cummings, Reading, MA, 1976).

[31] R.W. Goodby and R. Pindak, Mol. Cryst. Liq. Cryst. **75**, 233 (1981).